Current Biology, Vol. 14, 449–457, March 23, 2004, ©2004 Elsevier Ltd. All rights reserved. DOI 10.1016/j.cub.2004.03.006

Integration of Chemosensory Pathways in the *Drosophila* Second-Order Olfactory Centers

Nobuaki K. Tanaka,[1,2,3] Takeshi Awasaki,[1,3,4] Takashi Shimada,[1,5] and Kei Ito[1,3,4,5,*]
[1]Institute of Molecular and Cellular Biosciences
The University of Tokyo
Yayoi, Bunkyo-ku, Tokyo 113-0032
Japan
[2]The Graduate University for Advanced Studies
Myodaiji, Okazaki, Aichi 444-8585
Japan
[3]National Institute for Basic Biology
Myodaiji, Okazaki, Aichi 444-8585
Japan
[4]Precursory Research for Embryonic Science and Technology
Japan Science and Technology Agency
c/o Institute of Molecular and Cellular Biosciences
University of Tokyo
Yayoi, Bunkyo-ku, Tokyo 113-0032
Japan
[5]Institute for Bioinformatics Research and Development
Japan Science and Technology Agency
c/o Institute of Molecular and Cellular Biosciences
University of Tokyo
Yayoi, Bunkyo-ku, Tokyo 113-0032
Japan

Summary

Background: Behavioral responses to odorants require neurons of the higher olfactory centers to integrate signals detected by different chemosensory neurons. Recent studies revealed stereotypic arborizations of second-order olfactory neurons from the primary olfactory center to the secondary centers, but how third-order neurons read this odor map remained unknown.
Results: Using the *Drosophila* brain as a model system, we analyzed the connectivity patterns between second-order and third-order olfactory neurons. We first isolated three common projection zones in the two secondary centers, the mushroom body (MB) and the lateral horn (LH). Each zone receives converged information via second-order neurons from particular subgroups of antennal-lobe glomeruli. In the MB, third-order neurons extend their dendrites across various combinations of these zones, and axons of this heterogeneous population of neurons converge in the output region of the MB. In contrast, arborizations of the third-order neurons in the LH are constrained within a zone. Moreover, different zones of the LH are linked with different brain areas and form preferential associations between distinct subsets of antennal-lobe glomeruli and higher brain regions.
Conclusions: MB is known to be an indispensable site for olfactory learning and memory, whereas LH function is reported to be sufficient for mediating direct nonassociative responses to odors. The structural organization of second-order and third-order neurons suggests that MB is capable of integrating a wide range of odorant information across glomeruli, whereas relatively little integration between different subsets of the olfactory signal repertoire is likely to occur in the LH.

*Correspondence: itokei@iam.u-tokyo.ac.jp

Introduction

A smell usually comprises a mixture of odorants, which are initially detected by the array of olfactory receptor neurons (ORNs, also termed first-order olfactory neurons: Figure 1A) [1]. For the perception of a particular smell, information carried by each type of ORN must be integrated and then further categorized within the brain. ORNs expressing the same olfactory receptor send their axons to topographically fixed glomeruli in the primary olfactory center of the brain (olfactory bulb in mammals, antennal lobe [AL] in insects) [2–4]. Representation of odor at this level is thus a dynamic combination of active glomeruli [5–7].

Projection neurons (PNs, also termed second-order olfactory neurons, mitral/tufted cells in mammals, and projection neurons in insects) convey this information from AL glomeruli to secondary olfactory centers (e.g., piriform cortex, olfactory tubercle, and entorhinal cortex in mammals; mushroom body [MB] and lateral horn [LH] in insects, Figure 1A) [8, 9]. Because most PNs are uniglomerular and receive signals from a single type of ORNs, information detected by different ORN channels is not likely to be fully integrated at the level of the PNs. Supporting this contention, PN activities visualized by functional imaging [10–12] and with the recording of characteristic synchronized oscillatory spikes [13, 14] show a clear correlation between the ensemble of activated PNs and the types of odor applied.

Integration among different ORN channels must therefore occur in secondary or even higher-order olfactory centers. If we are to understand this process, we must gain important insight from the connectivity patterns, namely those between PNs and third-order neurons, in the next synaptic level of the olfactory pathway. The projection pattern of PNs has recently been reported both in mammals and insects [15–17]. In *Drosophila melanogaster*, for example, PNs from each glomerulus of the AL terminate in a stereotypic manner at the LH—one of the two target neuropils of the PNs [16, 17] (Figure 1B). The distribution of terminals in the other target—the calyx region of MB—is still unclear. The relationships between these PN terminals and the dendritic arborizations of third-order neurons of both LH and MB remain essentially unknown.

We here report the first systematic comparison of arborization patterns between PNs and third-order neurons. In the MB, they are organized such that the MB's output region (called lobes) can read olfactory information conveyed via all types of PNs. In the LH, however, third-order neurons link segregated subgroups of PNs

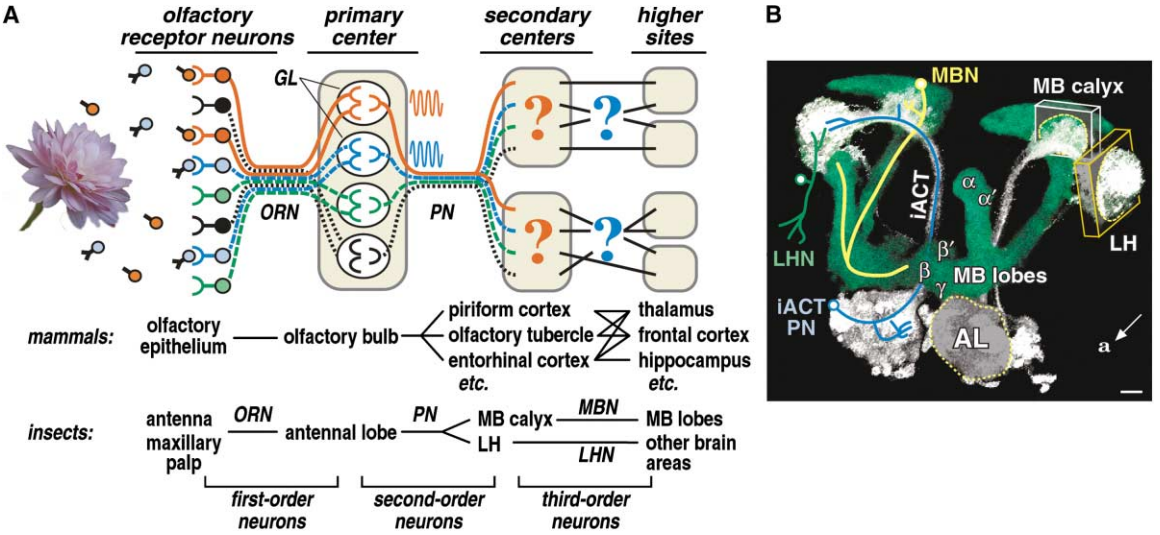

Figure 1. The Process of Odor Recognition

(A) Schema of olfactory pathway, which is consistent between mammals and insects. The odorants emitted by the object stimulate distinct subsets of olfactory receptor neurons (red and blue ones in this case), which terminate at specific glomeruli (GL) of the primary olfactory center. The information about the active glomeruli is transmitted to multiple secondary centers via projection neurons (PNs, second-order neurons). They terminate in the secondary centers in a stereotypic manner, but their spatial localizations are only partially understood. Almost no data are available about the connection patterns of the third-order neurons (question marks).

(B) Oblique view of the *Drosophila* olfactory pathway. Anterior (a) is to the lower left. Green signal represents the mushroom bodies (MB). The PNs of the inner antennocerebral tract (iACT PNs, white signal) connect the antennal lobe (AL) with the lateral horn (LH) and the calyx of the mushroom body (MB). The MB neuron (MBN) forms its dendritic arborization in the calyx and projects to the lobes (either α/β, α'/β', or γ). The LH neuron (LHN) connects the LH with various other sites of the brain. The yellow and white boxes represent the position and orientation of the LH and MB cross-sections shown in the following figures. The scale bar represents 20 μm.

exclusively with specific brain areas. This latter result is unexpected because it suggests the existence of parallel but separated channels between distinct subsets of olfactory sensory neurons and higher brain regions.

Results

Correlated Map of Projection Neuron Terminals between the Two Secondary Olfactory Centers

The first stage of this analysis was to establish a spatial map of the terminals of PNs in their two target neuropils, the LH and the calyx region of the MB. We analyzed PNs that send their axons through the inner antennocerebral tract (iACT, Figure 1B), one of three olfactory tracts arising from the antennal lobes and the only tract from which most PNs supply arborizations to both the LH and MB [8, 18].

Screening about 4,000 GAL4 enhancer-trap strains [19–21], we identified five lines that reproducibly revealed specific subsets of the iACT PNs. Three lines label PNs that have dendrites in only a single glomerulus (DL1, VA6, and VM2, respectively; Figure 2A). The other two lines label PNs whose uniglomerular dendrites contribute to triplets of glomeruli (DA1/DC3/VA1d and DM1/VA4/VC1, respectively). These PNs together label nine out of a total of 43 uniquely identifiable glomeruli [22].

To obtain precise comparisons between the brains of different individuals, we used specific landmarks to standardize the size and orientation of each specimen (see Figure S1 in the Supplemental Data available with this article online). When the LH was observed as a sagittal cross-section, the endings of PNs from a single glomerulus (DL1 and VA6) were seen to invade a small volume of it (Figure 2B, left). This distribution was consistent among individuals, as evidenced by the overlaid images from three preparations. The terminals of these two sets of PNs spatially overlap, suggesting that projections from more than one glomerulus converge to the same zone of the LH. This is further supported by observations of strains that label larger number of PNs. Those from the combination of three glomeruli DA1/DC3/VA1d all terminate in the same anterior-ventral LH area, distinct from the area invaded by terminals from DL1/VA6 as described above. Likewise, PNs from glomeruli VM2 and DM1/VA4/VC1 terminate in a posterior-dorsal area (Figure 2B, right), which has little spatial overlap with terminal areas of the other two sets of PNs.

To compare these observations more quantitatively, we took the intensity of pixels of each cross-sectional image as a vector. The image vectors of different individuals were clustered via the K-means algorithm ([23, 24]; see also Figure S2) to compare the Euclidean distances between vectors. The clustering demonstrates that PN terminals from the selected nine glomeruli clearly fall into three discrete classes (Figure 2D). These glomeruli can therefore be categorized into three functional groups according to the locations of their terminals in the LH (rightmost schema in Figure 2B).

Do the endings of PNs in the MB calyx analogously segregate? Although optical recordings from PNs [12] and Golgi impregnations [25] suggest that terminals might be stacked into discrete zones, previous studies

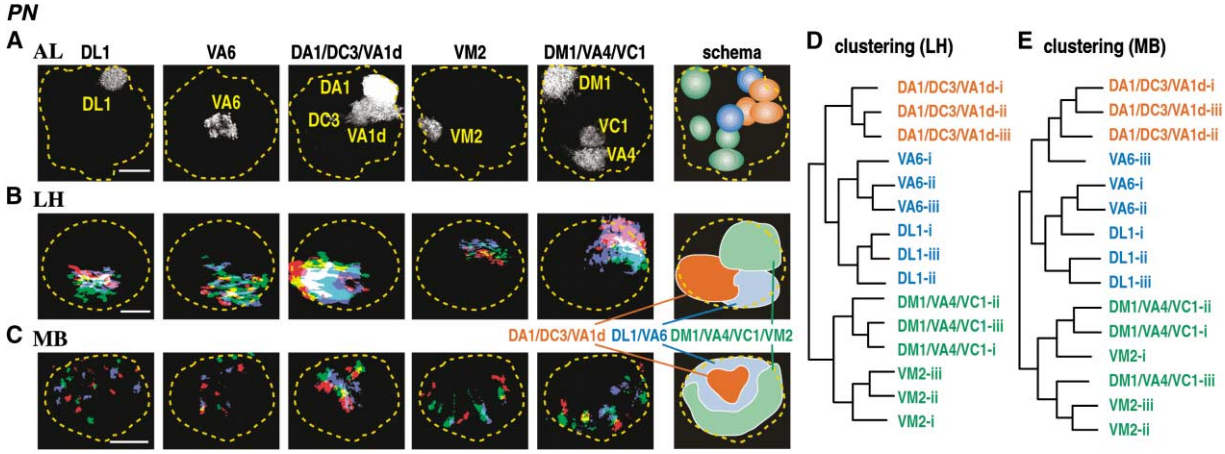

Figure 2. Projection Patterns of PNs

(A) Staining pattern of the five GAL4 strains in the AL cross-section. Frontal view. Dorsal is to the top, lateral is to the right. Dashed lines represent the outline of the AL. The names of the labeled glomeruli are shown in and above the figures. The rightmost panel is the schematic representation of the nine glomeruli labeled by these strains.

(B) Arborization patterns in the LH. A standardized sagittal cross-section of about a 20 μm thickness at the center of the LH was generated from the confocal stacks (yellow box in Figure 1B). Dorsal is to the top, and anterior is to the left. Sections of three individuals are overlaid (shown in red, green, and blue). The terminals of PNs arborize in three discrete subregions (rightmost schema).

(C) Standardized frontal cross-section of the MB calyx (white box in Figure 1B). Overlay of three individuals in three colors as in (B). Dashed lines indicate the outline of the calyx. The arborizations are spatially categorized into three layered zones (schema).

(D and E) Cluster analysis. The images of three individuals (with suffices -i, -ii, and -iii correspond to the red, green, and blue image, respectively) of five strains were compared via the K-means algorithm (Figure S2). The length of the horizontal bars reflects the degree of correlation between each cluster (relative "distance" between clusters).

comparing single neurons have not been able to identify clear patterning in this area [16, 17]. Our analysis demonstrated clear stereotyped zonal separations (Figure 2C). PNs from glomeruli DA1/DC3/VA1d arborize at the central zone of the calyx's cross-section. Arborizations from VM2 and from the combination of DM1/VA4/VC1 occupy the same ventral peripheral zone. Those from DL1/VA6 distribute in an intermediate area, although there is slight overlap between their area of arborization and the central and peripheral zones contributed by other PNs. Cluster analysis confirms this spatial segregation (Figure 2E), which is analogous to the pattern in the LH.

In summary, PNs from specific AL glomeruli supply distinct zones in both the LH and MB. In the MB, the zones occupy concentric layers, whereas in the LH they are clustered along the dorsoventral and anteroposterior axes (schema in Figures 2B and 2C, right). Despite topological differences, the two secondary olfactory centers confer comparable odor maps.

Arborizations of LH Neurons Restricted in the Discrete Zones of PN Terminals

The above results demonstrate that both the MB calyx and LH are divided into at least three zones based on the segregation of PN arborizations. Are these channels maintained as discrete entities, or are they intermingled at the level of the third-order neurons of the LH and MB?

To address this, we analyzed whether arborizations of the neurons of the LH (LH neurons: LHNs) and those of the MB (MB neurons: MBNs) are confined within a specific zone defined by PNs or extend across different zones. Because there are almost no descriptions of LHNs, we screened four thousand GAL4 strains to finally identify six LHN lines (Figure 3A). LHNs arborize in the LH and in remote cerebral neuropils. We identified three classes of them. The first class of LHNs arborizes dorsally in the LH (left three panels of Figure 3A, top), and its remote terminals arborize in the dorsal areas of the brain (superior medial protocerebrum [smpr] and superior lateral protocerebrum [slpr], Figure 3A, bottom). The second class arborizes only in the ventral LH, especially in its anterior region, and remotely innervates ventral brain neuropils (deutocerebrum's antennal mechanosensory and motor center [ammc] and areas of the ventrolateral protocerebrum [vlpr]). The third class has diffuse arborizations in the ventral LH, with a concentration of processes in its posterior zone. This type of cell connects the LH with areas of the lateral brain (vlpr and lateral protocerebrum [lpr]).

Cluster analysis reveals relationships between the terminals of PNs and the arborizations of these three classes of LHNs (Figure 3B). PN terminals from glomeruli DM1/VA4/VC1 and VM2 share the same field of arborization with LHNs that have remote connections to the dorsal brain (smpr and slpr). Terminals from glomeruli DA1/DC3/VA1d, and also from DL1/VA6, are preferentially associated with connections to the ventral and lateral brain regions.

In order to examine whether PNs and LHNs classified in the same cluster are directly connected, we visualized combinations of PNs and LHNs simultaneously in a single individual by crossing two GAL4 strains (Figure 3C). In the anterior ventral LH, the terminals of the PNs from DA1/DC3/VA1d intermingle with the arborization of the LHNs that remotely innervate the vlpr (Figure 3C1). Likewise, arborizations of the PNs from DM1/VA4/VC1 and

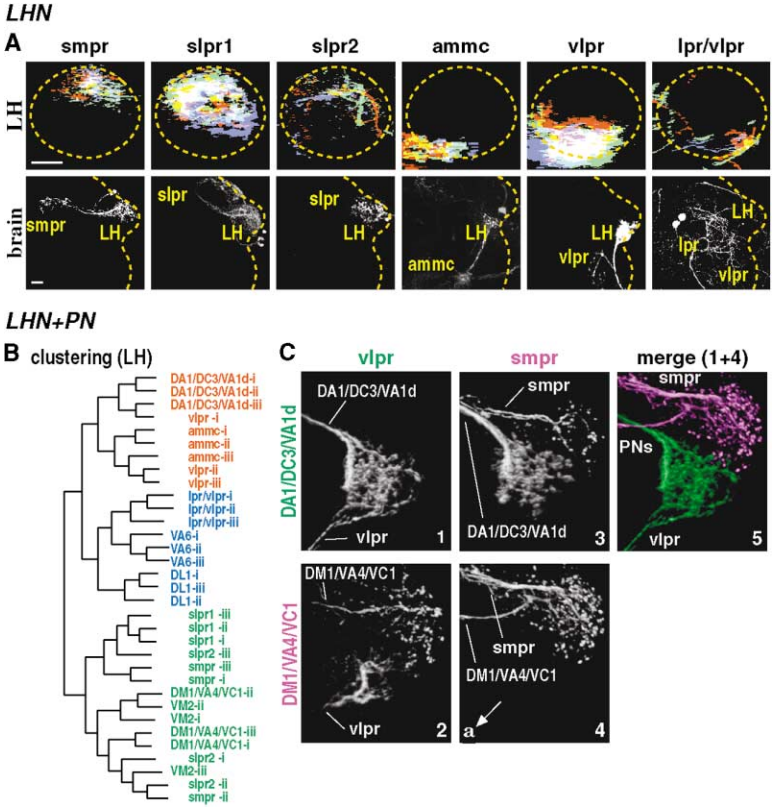

Figure 3. Spatial Correlation between LHNs and PNs

(A, top) Sagittal cross-section of the LH. Overlay of three individuals as in Figure 2B. Anterior is to the left. (A, bottom) Frontal view of the whole left protocerebrum. Dashed lines show the outline of the neuropil. Lateral is to the right. Six GAL4 strains clearly visualize various types of LHNs. The names of the brain regions that are connected with the labeled LHNs are shown on top and within the figure (bottom). Abbreviations are as follows: sm, superior medial; sl, superior lateral; vl, ventrolateral; l, lateral; pr, protocerebrum; ammc, antennal mechanosensory and motor center. Scale bars represent 20 μm.

(B) Combined cluster analysis of the six types of LHNs and the five types of PNs.

(C) Oblique view of the LH. Anterior (a) is to the lower left. PNs from DA1/DC3/VA1d and DM1/VA4/VC1 and LHNs that remotely innervate either vlpr or smpr are simultaneously labeled in four combinations (1–4) from a cross of two GAL4 strains. The size, position, and orientation of the images are standardized as in other figures. A merger of image 1 and image 4 is shown in 5.

those of the LHNs with their remote innervation in the smpr intermingle in the dorsal posterior LH (Figure 3C4). In both cases, close examination of the confocal serial sections showed that the branches of PNs and LHNs are labeled continuously, suggesting that they are in direct contact at least at the resolution of confocal sections (1 pixel = 0.3 μm). On the other hand, completely detached arborizations were observed when PNs and LHNs that belong to different clusters were visualized simultaneously (Figures 3C2 and 3C3).

From these results, we conclude that LHN arborizations are constrained within a zone defined by the endings of PNs from a specific subset of glomeruli. Unless there are indirect interzone interactions mediated by local neurons, each group of LHNs cannot alone read olfactory information from more AL glomeruli than are represented in their branching domain (Figure 3C5).

Arborizations of MB Neurons Covering Multiple Zones of PN Terminals

Does the MB calyx also possess functional subunits that are segregated like those in the LH? The calyx is densely invaded by the dendrites of MBNs, also known as Kenyon cells (Figure 1B) [25, 26]. MBNs send their axons to specific subdivisions of the lobes (e.g., γ, α′/β′, α/β lobes, Figure 1B) according to their birth order [27]. The neurons of the α/β lobes can further be divided into two types (core and surface) because many molecular markers label these separately [25]. We thus asked whether different lobes of the MB might receive olfactory information from different subsets of AL glomeruli.

Although the structures of different types of MBNs have been investigated in detail [25–31], whether the dendrites of MBNs contributing to each lobe occupy specific subregions of the calyx has not been understood clearly. We therefore screened GAL4 strains that selectively reveal MBNs innervating a single set of lobes (Figure 4A). The dendrites of the γ lobe MBNs preferentially, but not exclusively, occupy the center of the calyx (first panel of Figure 4A). Dendrites of other types of MBNs appear more widespread across the calyx, although the distribution is slightly nuanced.

We estimated whether this nuanced distribution of MBN dendrites spatially relates to zones defined by different PNs by calculating the "distances" (Figure S2) between image vectors for MBNs and PNs (Figure 4B). The γ lobe MBNs show a statistically more significant association with PNs from glomeruli DA1/DC3/VA1d ($p < 0.05$, asterisk in the first panel of Figure 4B). MBNs supplying the α′/β′ lobes and α/β lobes showed no significant correlation, leading to the conclusion that these lobes receive information from all nine glomeruli with essentially no preference (Figure 4B).

Correlation between MBNs and PNs at the Single-Cell Level

Fewer than 200 PNs innervate the calyx, whereas the number of MBNs is more than 2,500 [8, 32]. How, then, might each MBN collect information from PN collaterals? Unlike in the LH, the arborizations of each type of MBN collectively cross the border between the concen-

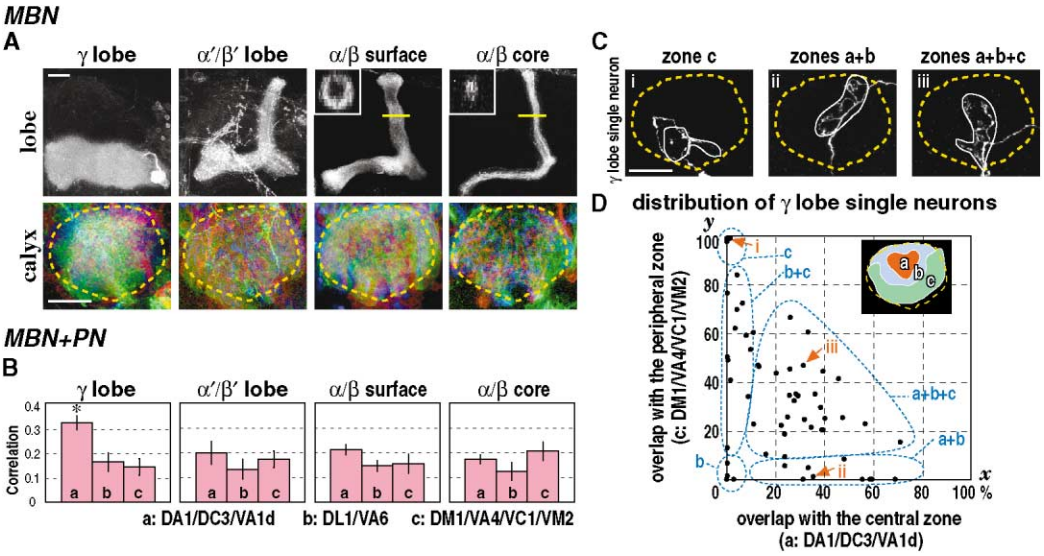

Figure 4. Spatial Correlation between MBNs and PNs

(A, top) MBNs that innervate the γ, α′/β′, and α/β lobes are selectively visualized by four GAL4 enhancer-trap strains. The neurons contributing the α/β lobes can be subdivided into two types, which contribute either the surface layer or the core of the lobe (inset: horizontal cross-section of the α lobe at the level shown by the yellow line). (A, bottom) Arborization pattern of each type of MBN in the calyx. Same view as in Figure 2C. An Overlay of three individuals shown in red, green, and blue.

(B) Spatial correlation between the arborizations of MBNs and three classes of PNs. The correlation was measured as the reciprocal of the mean "distance" between image vectors of MBNs and PNs (see Experimental Procedures). Longer bars mean shorter distance and thus stronger correlation. The error bar indicates the standard deviation of distances. An asterisk indicates $p < 0.05$.

(C) Arborizations of single γ lobe MBNs in the calyx. White lines mark the field of arborization. Zones a, b, and c represent the area of calyx cross-section contributed by the terminals of the three classes of PNs, respectively (inset of Figure 4D).

(D) Spatial overlap between single γ lobe neurons and the three zones defined by the PN terminals. For each image of 58 MBNs, the percentage of the pixels that fall within the central zone of the calyx (zone a, defined by the PNs from DA1/DC3/VA1d, *x* axis) and those within the peripheral zone (zone c, defined by the PNs from DM1/VA4/VC1/VM2, *y* axis) were calculated. The percentage (100-x-y) approximates the ratio of the pixels that fall in the intermediate zone (zone b). (Note that, because of the slight overlap with zones a and c, zone b is set smaller than the actual area contributed by the arborization of PNs from DL1/VA6.) If $x \approx 100\%$ or $y \approx 100\%$, the dot represents an MBN whose arborization is confined within zone a or zone c, respectively. If $x \approx 0\%$ and $y \approx 0\%$, it represents a neuron that arborizes only in zone b. If $x \approx 0\%$ and $y << 100\%$, the neuron arborizes in two zones (b + c), and if $x << 100\%$ and $y \approx 0\%$, the neuron sends its dendrites to zones (a + b). Finally, if x and y $<<$ 100% but they are significantly larger than 0%, the percentage (100-x-y) is also significantly larger than 0%. Such a dot represents a neuron that arborizes in all the three zones.

Scale bars represent 20 μm.

tric zonations defined by PNs. Does this imply that each MBN arborizes across these zones?

To study whether a single MBN arborizes within or across PN zones, we compared the dendrites of single γ lobe neurons visualized with the FRT-GAL4 [30] and MARCM [33] systems. There were MBNs arborizing within a single zone, in two zones, and across all the three zones (Figure 4C). We further analyzed the spatial relationship between MBNs and PN zones by calculating the overlap between the dendrites of 58 single γ lobe neurons and each of the three zones (Figure 4D). Among 58 cells examined, only seven cells had their dendrites confined in a single zone. Twenty-one cells extend their dendrites to two zones, and 30 cells innervate all the three zones. Although the overall density of dendrites is higher in the center of the calyx (zone A, Figures 4A and 4B, left), the group of MBNs innervating the same γ lobe is thus a heterogeneous population in respect to the correlation with the PN zones.

These data suggest that a single MBN receives signals from PNs representing either only one class of glomeruli or various combinations of them. A large number of these heterogeneous MBNs send their axons to the same lobe. As a consequence, each lobe of the MB could, in principle, integrate information sent to it from the entire AL.

Maintenance of Correlated Arborization Patterns without Olfactory Input

Are such characteristic relationships between PNs and third-order olfactory neurons (MBNs and LHNs) hard-wired, or might these be sustained and fine-tuned in an activity-dependent manner? These arborizations were patterned already at late pupal stages (up to 10 hr before eclosion, data not shown) essentially in the same way as in mature adult flies. Thus, they are established before animals experience the full variety of odors and are not subject to fine-tuning after eclosion. We further examined the consequence of a complete loss of olfactory sensory input by surgically removing all olfactory sensilla at the time of eclosion and then examining flies 14 days postoperatively. No differences in PNs, LHNs, or

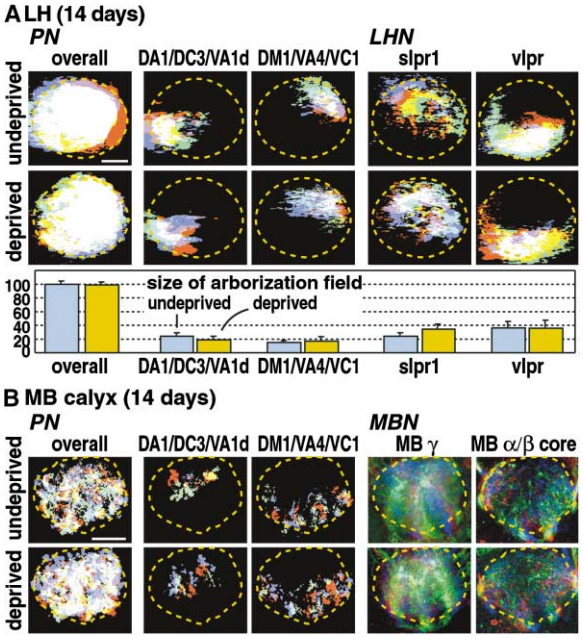

Figure 5. Invariant Arborization Pattern of PNs, LHNs, and MBNs after Surgical Deprivation of Olfactory Input

Both the antennae (the third and more distal segments) and maxillary palpi were cut out from the adult flies just after eclosion. Scale bars repersent 20 μm.

(A) Comparison of control and olfactory-deprived flies at the LH cross-section 14 days after eclosion. Overlay of three individuals. The graph compares the area of arborization in each cross-section. (The mean and standard deviation of three individuals are shown. The average area of the total LH cross-section is normalized to 100.)

(B) Comparison at the MB calyx cross-section.

MBNs were found between undeprived and deprived animals (Figure 5), nor was any retraction of fiber branches observed. These data suggest that not only stereotypic branching of PNs [16, 17] but also the structural correlation between PNs and third-order neurons are maintained even without olfactory input.

Discussion

Separated Channels of PNs

Here we analyzed the distribution of PN terminals in both secondary olfactory centers of *Drosophila*. As has been shown previously [16, 17], PNs have stereotypic arborizations in the LH. Comparing the localization of PN terminals in the cross-section, we revealed that there are at least three zones in the LH and that each of these receives different sets of olfactory input via PNs. Previous studies, which classified PNs according to their branching patterns [16, 17], did not identify zonations in the MB. The branching patterns of PNs are much more variable in the MB than in the LH (our unpublished data). The area of their arborizations, however, is strikingly consistent. By mapping these areas, we were able to identify clear concentric zones in the MB.

Because these zones receive information from different sets of AL glomeruli, a particular odor would evoke different activity between them. Indeed, optical imaging with a calcium-sensitive fluorescence reporter, *cameleon*, revealed different activity patterns between the center and periphery of the calyx [12].

The zonal projections identified in the LH and MB are highly correlated (Figure 6). This suggests that glomeruli in the AL can be categorized into discrete functional groups not only according to (1) the identity of the ORNs they receive [1, 3] (represented in alphabets A–I in Figure 6) but also (2) whether their PNs converge to the same or different zones of secondary olfactory centers (represented in three colors in Figure 6).

Connectivity between Second-Order and Third-Order Olfactory Neurons

In this study we tried to reveal the connectivity pattern between second-order olfactory neurons (PNs) and third-order olfactory neurons by comparing their area of arborizations. We identified combinations of PNs and LHNs that share the same arborization field in the LH. Simultaneous visualization of them showed that, at least in the cases we tested, the arborizations of these neurons contact with each other. This would strongly suggest that there are synaptic connections between them. Even in the case when they actually had intersected without making synapses, interaction between these intertwined arborizations would be much more intense than between the neurons whose arborizations are completely segregated (Figure 3C5).

Precise synaptic connection between PNs and third-order neurons could, in principle, be analyzed more directly via targeted expression of a *trans*-synaptic marker such as wheat germ agglutinin (WGA) [34]. The system, however, does not work reliably in most neurons of the *Drosophila* central brain, where WGA spreads into adjacent neurons nonspecifically (our unpublished data). Unless a more specific technique is developed, the approach we took in this study would be the best alternative.

Differences between the Neural Circuits of the Two Secondary Olfactory Centers

We showed that the distributions of PN terminals are essentially similar between the two secondary olfactory centers. Thus, the functional differences between these centers are likely to be reflected by the differences in how third-order neurons are associated with the zonal arborizations of PNs.

Behavioral and molecular analyses suggest that the information pathway involving the MB is crucial for the associative processing of olfactory signals [35–40]. MBNs have been suggested to function as coincidence detectors [41]. Although PNs convey activity information from a specific group of AL glomeruli to a specific zone of the MB calyx, dendrites of MBNs that contribute to each lobe collectively cover these zones. At the single-cell level, an MBN extends its dendrites either within a single zone or in two or three zones, suggesting that different MBNs would contact PNs from diverse combinations of glomeruli. Axons of this heterogeneous population of MBNs all converge at the lobe region. Thus, each lobe could, in principle, read information sent from the entire AL (Figure 6). Such convergence might be

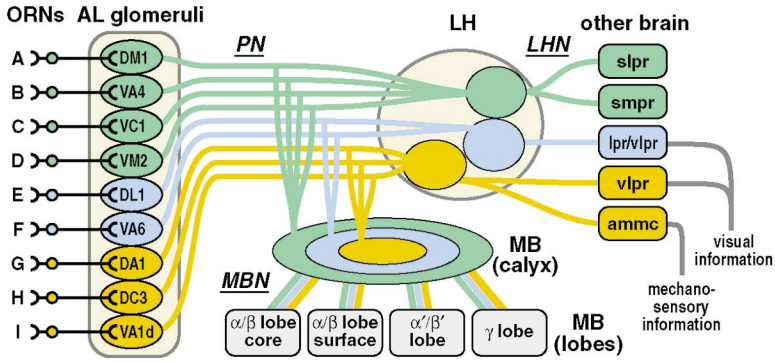

Figure 6. Schema of the Olfactory Pathways in the Fly Brain

Nine types of ORNs (tentatively labeled as A–I) innervate corresponding glomeruli of the AL. The PNs from these glomeruli converge to three discrete zones in the LH and MB calyx. The glomeruli and ORNs can thus be classified into three subgroups (indicated in three colors). The LHNs connect the zones of LH with different brain regions and thus form separated information channels between subtypes of ORNs and specific brain regions. Only regions linked with the ventral LH have direct associations with visual and mechanosensory pathways. The integration by the MBNs is more overlapping. Each MBN arborizes either within a particular zone or across zones. Collectively, the neurons in each MB lobe receive information from across the glomeruli.

important for the associative function of this olfactory center.

In the LH of the *Drosophila* brain, the arborizations of the third-order neurons were identified for the first time. We found that their arborizations are constrained within zones that are defined by PN terminals. Thus, each group of LHNs has access to only a limited repertoire of olfactory information. Furthermore, LHNs originating from different zones of the LH innervate different areas of the brain. One consequence of such connectivity pattern is the hitherto unexpected existence of separated parallel channels between olfactory sensory neurons and higher processing sites (Figure 6). These channels are made before eclosion and maintained without olfactory input. This might suggest that keeping such neural circuits would be important when insects mediate olfactory responses to odors they have never experienced.

The different zones of the LH are also associated with the sensory pathways of other modalities in a different way. The ventral region of LH is linked with the vlpr and ammc, which are, respectively, the major target of visual neurons from the optic lobe and the sole target of the mechanosensory antennal neurons, including the auditory sensory organ ([42] and our unpublished data). The brain regions connected with the dorsal LH, on the other hand, lack major input from the visual and mechanosensory pathways. There is thus a significant difference in the degree of sensory convergence between odorant information associated with the ventral and dorsal halves of the LH (Figure 6).

Information pathways via the LH must be sufficient for nonassociative odor-related behavior because the ablation of the MB causes no effect on these functions [43–45]. Structural organization of PNs and LHNs suggests that the LHNs and presumably higher centers in the brain linked with these segregated LH zones read only a subset of olfactory glomeruli. Such a limited level of integration seems sufficient for mediating animals' direct behavioral responses to odors.

From the sensory organs to the primary and secondary centers, the structure and topology of olfactory neural networks are strikingly similar between insects and mammals [46, 47]. Like information from the LH and MB of insects, information from a single type of mammalian ORN is conveyed to only a small part of each secondary center, such as the piriform cortex and olfactory tubercle [15]. If the similarity between insect and mammalian olfactory systems can further be extrapolated, similarly separated channels from the ORN to higher cortical areas might play important roles in mediating the direct olfactory response of mammals.

Conclusions

The present analysis has provided an important perspective about the structural relationships between second-order and third-order olfactory neurons of *Drosophila*. Arborizations of second-order neurons from distinct subgroups of AL glomeruli form essentially similar zonations in the two secondary olfactory centers, the LH and MB. In the MB, which is important for olfactory learning and memory, dendrites of third-order neurons show diverse distributions across zones. Axons of these heterogeneous neurons converge at each MB lobe, suggesting that extensive integration across a wide range of olfactory signals would occur. In the LH, which is important for immediate responses to odors, arborization of each type of third-order neurons is limited within one of these zones, suggesting limited integration among small subsets of odorant repertoire. Further physiological analyses of the uniquely identified second- and third-order neurons will provide vital information for understanding how olfactory information is received and integrated in the two secondary olfactory centers.

Experimental Procedures

Drosophila Strains Used for Labeling Cells

To label specific neurons in the olfactory pathway, we screened in total 3,939 GAL4 enhancer-trap strains made by the laboratory of G.M. Technau (MZ series) [48] and by the NP consortium (NP series) [19, 20]. The original names of the strains and the average number and standard deviation of labeled PNs are as follows: DL1 (NP3529, 2.0 ± 0.0), VA6 (NP80, 1.0 ± 0.0), DA1/DC3/VA1d (MZ19, 13.4 ± 1.5), VM2 (NP5103, 2.0 ± 0.0), DM1/VA4/VC1 (NP5221, 3.5 ± 0.6), smpr (MZ671, 3.0 ± 1.0), slpr1 (NP6099, 3.3 ± 0.6), slpr2 (NP3060, 2.3 ± 0.6), ammc (NP1004, 7.7 ± 1.5), vlpr (NP5194, 12.3 ± 1.5), lpr/vlpr (NP10, 1.0 ± 0.0), γ lobe (NP21, approximately 200), α′/β′ lobe (NP65, approximately 100), α/β surface (NP5286, approximately 500), α/β core (NP7175, 58 ± 12), and overall PN (NP225, 70 ± 3

cells, which contribute 35 out of the total 43 glomeruli). Single-cell labeling of MBNs (Figures 4C and 4D) was performed with both FRT-GAL4 [30] and MARCM [33] systems.

Visualization and Standardization of Brain Preparations

The brains of female flies between 4 and 10 days after eclosion (14 days in case of ablation experiment) were dissected, fixed, and stained with rat polyclonal anti mouse-CD8 α-subunit antibody (diluted at 1:200; from Caltag), mouse monoclonal antibody nc82 (gift from E. Buchner and A. Hofbauer, 1:10), and Cy3-conjugated anti-rat or mouse secondary antibodies (Jackson, 1:200). Confocal serial optical sections at 0.9 μm intervals were taken with LSM 510 confocal microscopes (Zeiss) and water-immersion 40$\times$ Plan-Apochromat objective lenses (in most cases, frontal sections were taken from the rear side of the brain) and processed with the 3D reconstruction software Imaris 2.7 (BitPlane) running on Silicon Graphics Octane2 workstations and Volocity 2.5 (Improvision) on Macintosh computers.

For precise comparison of the region of innervation visualized among different individuals, it was necessary to compensate for the differences in size and orientation of the brain preparations. For this, the flies carrying two reporter genes (UAS-mCD8::GFP [33] and UAS-GFP S65T [T10], gift from Barry Dickson) were always used. GAL4-expressing cells were detected by the signal of anti-mCD8 antibody. Because UAS-GFP (T10) constitutively labels a large subset of MBNs regardless of GAL4 expression, the GFP signal was used to determine the positions of the calyx, pedunculus, and α lobe (See Figure S1). The transmission Nomarski images were taken simultaneously so that the edges of the brain neuropil and the outline of the calyx could be determined. These landmarks were used for adjusting the orientation of the 3D voxel data. The above landmarks were used for selecting the regions of the LH and MB cross-sections (white boxes in Figures S1B and S1D). The resulting images were then adjusted to defined size with Photoshop 7.0 (Adobe). For clarity, signals of glial cells, as well as those of neurons that are not related to the olfactory pathway, were removed from the final images.

Correlation Analysis and Clustering

The pixel values of the cross-section images of the LH and MB, after coarse-graining and intensity normalization, were regarded as the coordinate of a vector. The similarity between images can be evaluated with the distances between image vectors (Figure S2). For cluster analysis (Figures 2D, 2E, and 3B), images of three individuals per strain were compared. All the image vectors were initially regarded as a single cluster and then recursively divided into two clusters by the K-means algorithm (Figure S2C) [23, 24]. The obtained clustering tree was visualized with NJplot [49].

The correlation between the arborizations of MBNs and PNs (Figure 4B) was assessed from a calculation of the average of distances between three image vectors of MBNs and three or six PN vectors that fall in the same cluster of Figure 2E (in total, 9 or 18 combinations per each pair).

Distribution Analysis of a Single MBN

For examination of the distribution of arborization of a single MBN in association with the functional groups of PNs (Figure 4D), three concentric zones were first determined from the overlapping images of the PNs (inset in Figure 4D, which is identical with the rightmost schema of Figure 2C). For each image of the MBN single clone, the number of pixels that fall within central or peripheral zones was counted and divided with the total number of labeled pixels. A neuron was provisionally categorized as contributing to a particular zone if more than 8% of its pixels falls into that area.

Supplemental Data

Two supplemental figures are available with this article online at http://www.current-biology.com/cgi/content/full/14/6/449/DC1/.

Acknowledgments

We thank J. Urban and G. Technau for MZ series enhancer-trap strains, the members of the NP consortium and D. Yamamoto for the NP series strains, E. Buchner and A. Hofbauer for nc82 antibody, and the Bloomington stock center for UAS reporter strains. We are deeply indebted to M. Katsuki and T. Yamamori for their generous support at the National Institute for Basic Biology. We thank H. Otsuna and R. Okada for helpful discussions and sharing unpublished data, C. O'Kane and Y. Hiromi for critically reading the manuscript, and A. Hattori and N. Nishimura for technical assistance. This work was supported by Precursory Research for Embryonic Science and Technology/Japan Science and Technology Agency and Institute for Bioinformatics Research and Development/Japan Science and Technology Agency grants and Human Frontier Science Program (RG0134/1999-B) to K.I., a Precursory Research for Embryonic Science and Technology/Japan Science and Technology Agency grant to T.A., and by a Grant-in-Aid for Scientific Research to K.I. from the Ministry of Education, Culture, Sports, Science, and Technology of Japan.

Received: November 8, 2003
Revised: January 22, 2004
Accepted: January 22, 2004
Published: March 23, 2004

References

1. de Bruyne, M., Foster, K., and Carlson, J.R. (2001). Odor coding in the *Drosophila* antenna. Neuron *30*, 537–552.
2. Ressler, K.J., Sullivan, S.L., and Buck, L.B. (1994). Information coding in the olfactory system: evidence for a stereotyped and highly organized epitope map in the olfactory bulb. Cell *79*, 1245–1255.
3. Vosshall, L.B., Wong, A.M., and Axel, R. (2000). An olfactory sensory map in the fly brain. Cell *102*, 147–159.
4. Mombaerts, P., Wang, F., Dulac, C., Chao, S.K., Nemes, A., Mendelsohn, M., Edmondson, J., and Axel, R. (1996). Visualizing an olfactory sensory map. Cell *87*, 675–686.
5. Rubin, B.D., and Katz, L.C. (1999). Optical imaging of odorant representations in the mammalian olfactory bulb. Neuron *23*, 499–511.
6. Uchida, N., Takahashi, Y.K., Tanifuji, M., and Mori, K. (2000). Odor maps in the mammalian olfactory bulb: domain organization and odorant structural features. Nat. Neurosci. *3*, 1035–1043.
7. Galizia, C.G., and Menzel, R. (2000). Odour perception in honeybees: coding information in glomerular patterns. Curr. Opin. Neurobiol. *10*, 504–510.
8. Stocker, R.F. (1994). The organization of the chemosensory system in *Drosophila melanogaster*: a review. Cell Tissue Res. *275*, 3–26.
9. Shepherd, G.M. (1998). The synaptic organization of the Brain (Oxford University Press).
10. Wang, J.W., Wong, A.M., Flores, J., Vosshall, L.B., and Axel, R. (2003). Two-photon calcium imaging reveals an odor-evoked map of activity in the fly brain. Cell *112*, 271–282.
11. Ng, M., Roorda, R.D., Lima, S.Q., Zemelman, B.V., Morcillo, P., and Miesenbock, G. (2002). Transmission of olfactory information between three populations of neurons in the antennal lobe of the fly. Neuron *36*, 463–474.
12. Fiala, A., Spall, T., Diegelmann, S., Eisermann, B., Sachse, S., Devaud, J.M., Buchner, E., and Galizia, C.G. (2002). Genetically expressed cameleon in *Drosophila melanogaster* is used to visualize olfactory information in projection neurons. Curr. Biol. *12*, 1877–1884.
13. Laurent, G. (1999). A systems perspective on early olfactory coding. Science *286*, 723–728.
14. Kashiwadani, H., Sasaki, Y.F., Uchida, N., and Mori, K. (1999). Synchronized oscillatory discharges of mitral/tufted cells with different molecular receptive ranges in the rabbit olfactory bulb. J. Neurophysiol. *82*, 1786–1792.
15. Zou, Z., Horowitz, L.F., Montmayeur, J.P., Snapper, S., and Buck, L.B. (2001). Genetic tracing reveals a stereotyped sensory map in the olfactory cortex. Nature *414*, 173–179.
16. Marin, E.C., Jefferis, G.S., Komiyama, T., Zhu, H., and Luo, L. (2002). Representation of the glomerular olfactory map in the *Drosophila* brain. Cell *109*, 243–255.

17. Wong, A.M., Wang, J.W., and Axel, R. (2002). Spatial representation of the glomerular map in the *Drosophila* protocerebrum. Cell *109*, 229–241.
18. Stocker, R.F., Lienhard, M.C., Borst, A., and Fischbach, K.F. (1990). Neuronal architecture of the antennal lobe in *Drosophila melanogaster*. Cell Tissue Res. *262*, 9–34.
19. Yoshihara, M., and Ito, K. (2000). Improved Gal4 screening kit for large-scale generation of enhancer-trap strains. Drosoph. Inf. Serv. *83*, 199–202.
20. Hayashi, S., Ito, K., Sado, Y., Taniguchi, M., Akimoto, A., Takeuchi, H., Aigaki, T., Matsuzaki, F., Nakagoshi, H., Tanimura, T., et al. (2002). GETDB, a database compiling expression patterns and molecular locations of a collection of Gal4 enhancer traps. Genesis *34*, 58–61.
21. Brand, A.H., and Perrimon, N. (1993). Targeted gene expression as a means of altering cell fates and generating dominant phenotypes. Development *118*, 401–415.
22. Laissue, P.P., Reiter, C., Hiesinger, P.R., Halter, S., Fischbach, K.F., and Stocker, R.F. (1999). Three-dimensional reconstruction of the antennal lobe in *Drosophila melanogaster*. J. Comp. Neurol. *405*, 543–552.
23. Faber, V. (1994). Clustering and the continuous k-means algorithm. Los Alamos Sci. *22*, 138–144.
24. MacQueen, J. (1967). Some methods for classification and analysis of multivariate observations. Proc. Fifth Berkeley Symp. on Mathematical Statistics and Probability 281–297.
25. Strausfeld, N.J., Sinakevitch, I., and Vilinsky, I. (2003). The mushroom bodies of *Drosophila melanogaster*: an immunocytological and golgi study of Kenyon cell organization in the calyces and lobes. Microsc. Res. Tech. *62*, 151–169.
26. Yasuyama, K., Meinertzhagen, I.A., and Schurmann, F.W. (2002). Synaptic organization of the mushroom body calyx in *Drosophila melanogaster*. J. Comp. Neurol. *445*, 211–226.
27. Lee, T., Lee, A., and Luo, L. (1999). Development of the *Drosophila* mushroom bodies: sequential generation of three distinct types of neurons from a neuroblast. Development *126*, 4065–4076.
28. Jefferis, G.S., Marin, E.C., Watts, R.J., and Luo, L. (2002). Development of neuronal connectivity in *Drosophila* antennal lobes and mushroom bodies. Curr. Opin. Neurobiol. *12*, 80–86.
29. Zhu, S., Chiang, A.S., and Lee, T. (2003). Development of the *Drosophila* mushroom bodies: elaboration, remodeling and spatial organization of dendrites in the calyx. Development *130*, 2603–2610.
30. Ito, K., Awano, W., Suzuki, K., Hiromi, Y., and Yamamoto, D. (1997). The *Drosophila* mushroom body is a quadruple structure of clonal units each of which contains a virtually identical set of neurones and glial cells. Development *124*, 761–771.
31. Crittenden, J.R., Skoulakis, E.M., Han, K.A., Kalderon, D., and Davis, R.L. (1998). Tripartite mushroom body architecture revealed by antigenic markers. Learn. Mem. *5*, 38–51.
32. Technau, G., and Heisenberg, M. (1982). Neural reorganization during metamorphosis of the corpora pedunculata in *Drosophila melanogaster*. Nature *295*, 405–407.
33. Lee, T., and Luo, L. (1999). Mosaic analysis with a repressible cell marker for studies of gene function in neuronal morphogenesis. Neuron *22*, 451–461.
34. Yoshihara, Y., Mizuno, T., Nakahira, M., Kawasaki, M., Watanabe, Y., Kagamiyama, H., Jishage, K., Ueda, O., Suzuki, H., Tabuchi, K., et al. (1999). A genetic approach to visualization of multisynaptic neural pathways using plant lectin transgene. Neuron *22*, 33–41.
35. Roman, G., and Davis, R.L. (2001). Molecular biology and anatomy of *Drosophila* olfactory associative learning. Bioessays *23*, 571–581.
36. Heisenberg, M., Borst, A., Wagner, S., and Byers, D. (1985). *Drosophila* mushroom body mutants are deficient in olfactory learning. J. Neurogenet. *2*, 1–30.
37. Heisenberg, M. (2003). Mushroom body memoir: from maps to models. Nat. Rev. Neurosci. *4*, 266–275.
38. Dubnau, J., Grady, L., Kitamoto, T., and Tully, T. (2001). Disruption of neurotransmission in *Drosophila* mushroom body blocks retrieval but not acquisition of memory. Nature *411*, 476–480.
39. McGuire, S.E., Le, P.T., and Davis, R.L. (2001). The role of *Drosophila* mushroom body signaling in olfactory memory. Science *293*, 1330–1333.
40. Schwaerzel, M., Heisenberg, M., and Zars, T. (2002). Extinction antagonizes olfactory memory at the subcellular level. Neuron *35*, 951–960.
41. Perez-Orive, J., Mazor, O., Turner, G.C., Cassenaer, S., Wilson, R.I., and Laurent, G. (2002). Oscillations and sparsening of odor representations in the mushroom body. Science *297*, 359–365.
42. Strausfeld, N.J. (1976). Atlas of an Insect Brain (Berlin/Heidelberg/New York/Tokyo: Springer-Verlag).
43. de Belle, J.S., and Heisenberg, M. (1994). Associative odor learning in *Drosophila* abolished by chemical ablation of mushroom bodies. Science *263*, 692–695.
44. Heimbeck, G., Bugnon, V., Gendre, N., Keller, A., and Stocker, R.F. (2001). A central neural circuit for experience-independent olfactory and courtship behavior in *Drosophila melanogaster*. Proc. Natl. Acad. Sci. USA *98*, 15336–15341.
45. Kido, A., and Ito, K. (2002). Mushroom bodies are not required for courtship behavior by normal and sexually mosaic *Drosophila*. J. Neurobiol. *52*, 302–311.
46. Hildebrand, J.G., and Shepherd, G.M. (1997). Mechanisms of olfactory discrimination: converging evidence for common principles across phyla. Annu. Rev. Neurosci. *20*, 595–631.
47. Korsching, S. (2002). Olfactory maps and odor images. Curr. Opin. Neurobiol. *12*, 387–392.
48. Ito, K., Urban, J., and Technau, G.M. (1995). Distribution, classification, and development of *Drosophila* glial cells in the late embryonic and early larval ventral nerve cord. Roux. Archiv. Dev. Biol. *204*, 284–307.
49. Perriere, G., and Gouy, M. (1996). WWW-query: an on-line retrieval system for biological sequence banks. Biochimie *78*, 364–369.